



HAL
open science

Whole-genome mapping of 5' RNA ends in bacteria by tagged sequencing: a comprehensive view in *Enterococcus faecalis*.

Nicolas Innocenti, Monica Golumbeanu, Aymeric Fouquier d'Hérouël, Caroline Lacoux, Rémy A Bonnin, Sean P Kennedy, Françoise Wessner, Pascale Serror, Philippe Bouloc, Francis Repoila, et al.

► To cite this version:

Nicolas Innocenti, Monica Golumbeanu, Aymeric Fouquier d'Hérouël, Caroline Lacoux, Rémy A Bonnin, et al.. Whole-genome mapping of 5' RNA ends in bacteria by tagged sequencing: a comprehensive view in *Enterococcus faecalis*.. *RNA*, 2015, 21 (5), pp.1018-30. 10.1261/rna.048470.114 . hal-01464834

HAL Id: hal-01464834

<https://hal.science/hal-01464834v1>

Submitted on 24 Apr 2020

HAL is a multi-disciplinary open access archive for the deposit and dissemination of scientific research documents, whether they are published or not. The documents may come from teaching and research institutions in France or abroad, or from public or private research centers.

L'archive ouverte pluridisciplinaire **HAL**, est destinée au dépôt et à la diffusion de documents scientifiques de niveau recherche, publiés ou non, émanant des établissements d'enseignement et de recherche français ou étrangers, des laboratoires publics ou privés.



Distributed under a Creative Commons Attribution - NonCommercial 4.0 International License

METHOD

Whole-genome mapping of 5' RNA ends in bacteria by tagged sequencing: a comprehensive view in *Enterococcus faecalis*

NICOLAS INNOCENTI,^{1,2,3} MONICA GOLUMBEANU,^{4,5} AYMERIC FOUQUIER D'HÉROUËL,^{1,6} CAROLINE LACOUX,^{2,3} RÉMY A. BONNIN,⁷ SEAN P. KENNEDY,⁸ FRANÇOISE WESSNER,^{2,3} PASCALE SERROR,^{2,3} PHILIPPE BOULOC,⁷ FRANCIS REPOILA,^{2,3} and ERIK AURELL^{1,9}

¹Department of Computational Biology, KTH Royal Institute of Technology, AlbaNova University Center, SE-10691 Stockholm, Sweden

²INRA, UMR1319 Micalis, Domaine de Vilvert, F-78352, Jouy-en-Josas, France

³AgroParisTech, UMR Micalis, Domaine de Vilvert, F-78350, Jouy-en-Josas, France

⁴Department of Biosystems Science and Engineering, ETH Zürich, CH-4058, Basel, Switzerland

⁵SIB Swiss Institute of Bioinformatics, University of Basel, CH-4056, Basel, Switzerland

⁶Luxembourg Centre for Systems Biomedicine, University of Luxembourg, L-4362, Esch-sur-Alzette, Luxembourg

⁷Institut de Génétique et Microbiologie, Université Paris-Sud, CNRS, UMR8621, F-91405, Orsay, France

⁸INRA, MetaGenoPolis US1367, Domaine de Vilvert, F-78350, Jouy-en-Josas, France

⁹Department of Information and Computer Science, Aalto University, FI-02150 Espoo, Finland

ABSTRACT

Enterococcus faecalis is the third cause of nosocomial infections. To obtain the first snapshot of transcriptional organizations in this bacterium, we used a modified RNA-seq approach enabling to discriminate primary from processed 5' RNA ends. We also validated our approach by confirming known features in *Escherichia coli*. We mapped 559 transcription start sites (TSSs) and 352 processing sites (PSSs) in *E. faecalis*. A blind motif search retrieved canonical features of SigA- and SigN-dependent promoters preceding transcription start sites mapped. We discovered 85 novel putative regulatory RNAs, small- and antisense RNAs, and 72 transcriptional antisense organizations. Presented data constitute a significant insight into bacterial RNA landscapes and a step toward the inference of regulatory processes at transcriptional and post-transcriptional levels in a comprehensive manner.

Keywords: primary RNA; processed RNA; promoter; RNA degradation; *Enterococcus faecalis*

INTRODUCTION

Enterococcus faecalis is a ubiquitous Gram-positive bacterium and one of the first colonizers of the human gastro-intestinal tract after birth. It belongs to the core-microbiota and lives in the guts during the entire human life, suggesting a contribution of the bacterium to intestinal homeostasis (Campeotto et al. 2007; Adlerberth and Wold 2009; Qin et al. 2010). In contrast to this potentially beneficial role, *E. faecalis* is also the third cause of nosocomial infections and may carry and transfer various antibiotic resistances to other bacterial species, making its presence in the medical environment a seri-

ous concern (Arias and Murray 2012). The opportunism of *E. faecalis*, i.e., the transition from commensalism to pathogenicity in response to environmental cues, underlines its capacity to adapt to and survive in harsh conditions. Thus, deciphering the regulatory pathways that enable *E. faecalis* to undergo the transition from commensalism to pathogeny is a key component in the understanding the dual lifestyle of this microorganism (Gilmore and Ferretti 2003). The V583 strain was one of the first discovered vancomycin-resistant clinical isolates of *E. faecalis* (Sahm et al. 1989). Its genome, a circular chromosome (3218 kbp) and three circular plasmids pTEF1 (66 kbp), pTEF2 (57.7 kbp), and pTEF3 (18 kbp), contains at least 3264 annotated protein-coding genes (Paulsen et al. 2003). Although partial transcriptomic

Abbreviations: asRNA, antisense RNA; BHI, brain-heart infusion; dRNA-seq, differential RNA-seq; IGR, intergenic region; ORF, open reading frame; ppRNome, primary and processed transmission; PSS, processing site; PTS, phosphor-sugar transfer systems; RNA-seq, RNA sequencing; Sdh, serine-dehydratase; sRNA, small RNA; TSS, transcription start site; UTR, untranslated region

Corresponding authors: francis.repoila@jouy.inra.fr, eaurell@kth.se

Article published online ahead of print. Article and publication date are at <http://www.rnajournal.org/cgi/doi/10.1261/rna.048470.114>.

© 2015 Innocenti et al. This article is distributed exclusively by the RNA Society for the first 12 months after the full-issue publication date (see <http://rnajournal.cshlp.org/site/misc/terms.xhtml>). After 12 months, it is available under a Creative Commons License (Attribution-NonCommercial 4.0 International), as described at <http://creativecommons.org/licenses/by-nc/4.0/>.

analyses have been performed (Vebø et al. 2009, 2010; Aakra et al. 2010; Opsata et al. 2011), a comprehensive and dynamic view of the RNA landscape of V583 is missing.

Whole-transcriptome studies of prokaryotes via tiling arrays and RNA sequencing (RNA-seq) have unveiled a plethora of actively transcribed RNAs, and highly complex transcriptional organizations due to numerous promoters nested in open reading frames (ORFs), antisense (asRNAs) and small RNAs (sRNAs) genes (among other reviews Toledo-Arana and Solano 2010; Georg and Hess 2011). These global studies have been extremely valuable in determining transcribed regions in bacterial genomes and comparing RNA expression levels between different physiological states. Yet, their functional and regulatory insights remain incomplete as primary and processed RNAs cannot be distinguished and hence transcriptional (RNA synthesis) and post-transcriptional processes (RNA processing and stability) cannot be separated. The use of differential RNA-seq (dRNA-seq), an astute method that enriches an RNA population for primary transcripts, partially overcomes these limitations and gives access to the primary transcriptome (Albrecht et al. 2010; Bohn et al. 2010; Irnov et al. 2010; Sharma et al. 2010; Conway et al. 2014; Thomason et al. 2015). Yet, a major limitation of dRNA-seq is that all transcripts cannot be detected in a single experiment as they are degraded by a 5'-phosphate-dependent exonuclease, and thus information on post-transcriptional events is lost (Sharma et al. 2010). Global scale analysis of RNA stability has been performed in a few bacterial species, e.g., *Bacillus cereus* (Kristoffersen et al. 2012), *Bacillus subtilis* (Hambraeus et al. 2003), *Escherichia coli* (Selinger et al. 2003; Mohanty and Kushner 2006; Esquerré et al. 2013), *Mycobacterium tuberculosis* (Rustad et al. 2013), *Lactococcus lactis* (Redon et al. 2005), and *Prochlorococcus* (Steglich et al. 2010). These stability analyses have highlighted the broad and crucial contribution of RNA stability to gene expression reprogramming when bacteria face stresses, adapt to novel nutrient conditions, or grow at different rates. Those analyses consider transcribed regions as unique entities, where different sorts of RNA molecules can be present and cannot be seen.

We previously described a method that enables us to differentially tag 5' ends of primary and processed RNAs (Fouquier d'Hérouël et al. 2011). In the present work, we have coupled this method to RNA-seq, yielding novel insights into the bacterial RNA landscape where the primary and the processed transcriptomes (ppRNome) are unveiled within a single experiment. We have sorted transcription start sites (TSSs) and processing sites (PSSs) and validated the method by reproducing known results for *E. coli*.

The presented data provide a first snapshot of the RNA landscape of the human pathogen *E. faecalis*.

RESULTS AND DISCUSSION

Global view of the *E. faecalis* RNA landscape

Bacterial native (or primary) transcripts undergo cleavage that can be maturation or degradation processes (Rochat et al. 2013). Without the ability to identify and discriminate primary from processed transcripts, we have only partial information of gene expression control at the genome scale.

We have developed a method combining our previously introduced 5' RNA end tagging (Fouquier d'Hérouël et al. 2011) with deep sequencing technologies and termed it "tagRNA-seq" to visualize the primary and processed transcripts of *E. faecalis* in a genome-wide manner (Fig. 1; Supplemental Table SA and "The ppRNome browser" website, see "Visualization of Results" in Materials and Methods).

TagRNA-seq was performed on total RNAs extracted from bacteria grown in static (S) and respiratory (R) conditions, providing transcriptomes coined "St" and "Rt," respectively (Supplemental Section S2, Table S1). In parallel to these, and as control, three other RNA libraries from *E. faecalis* and one from *E. coli* were sequenced on different next-generation sequencing platforms (see Materials and Methods; Supplemental Section S2). Globally, St and Rt show that significant transcription occurs in a limited portion of the *E. faecalis* genome. Out of the 3.34 Mbp long genome, 1.65 Mbp appears to be transcribed in each condition (coverage >2×), including 90 kbp due to antisense transcription and 470 kbp made up by nonannotated and/or noncoding portions, i.e., 5'- and 3'-untranslated regions (UTRs), unannotated ORFs, and as- and sRNAs (see below). These data are

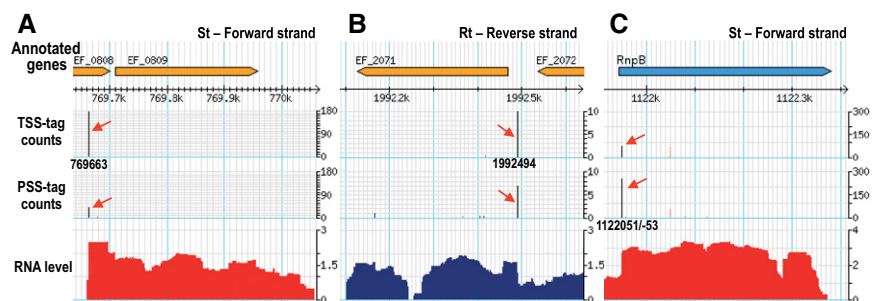


FIGURE 1. Three examples of 5' RNA ends viewed by tagRNA-seq on the *E. faecalis* V583 chromosome from the "ppRNome" browser. Below the line "Annotated genes," coordinates are those of the chromosome. The location of tags detected is indicated by the black vertical lines and the red arrows. TSS-tags are shown in the upper line, PSS-tags in the line below. "RNA levels" show the RNA signal detected; in red from St, in blue from Rt. Accurate values obtained for TSS- and PSS-tag counts and RNA levels are provided in Supplemental Table SA. (A) Transcription start site mapped at 769663/-5 for *ef0809*. This TSS could be easily predicted from the signal coverage. (B) TSS mapped at 1992494 for *ef2071*. This TSS is internal to the signal provided by the transcription of *ef2072* and would be difficult to predict. (C) Processing site mapped at 1,121,951/-53 for the RNA RnpB. This PSS is a dozen nucleotides downstream from the previously mapped TSS (see "Processing sites").

in line with previous reports highlighting that the information provided by annotations of bacterial genomes on their gene content remains incomplete (Toledo-Arana et al. 2009; Albrecht et al. 2010; Irnov et al. 2010; Sharma et al. 2010; Mitschke et al. 2011; Wurtzel et al. 2012; Conway et al. 2014; Thomason et al. 2015).

The calling of TSS and PSS from tagRNA-seq

We compared deep-sequencing data obtained with tagged and untagged RNA libraries prepared from *E. faecalis* grown in S conditions. Predictions of 5' edges based on sequence coverage signals from both libraries show good agreement, indicating that the tagging procedure does not alter the allocated coverage nor the location of putative transcription starts (Supplemental Section S3, Figure S3; the ppRNome browser). Several TSSs mapped previously by other methods were retrieved by tagRNA-seq at near-identical locations (± 2 bp) attesting to the reliability of the method. For example, we find the TSSs of *sodA* (*ef0463*), coding for the superoxide dismutase, *ptb* (*ef1663*), coding for the phosphotransbutyrylase, *fsrB/D* (*ef1821*), coding for the cysteine protease-like processing enzyme FsrB and the autoinducing propeptide FsrD of the *fsr* system, a homolog of the accessory gene regulator (*agr*) of *Staphylococcus aureus*, and *gelE* (*ef1818*), coding for a gelatinase (Qin et al. 2000, 2001; Ward et al. 2000; Nakayama et al. 2006; Verneuil et al. 2006) (see below; Supplemental Table SB).

In the ideal case, the procedure should identify unambiguously TSSs and PSSs. In practice, a fraction of 5' ends attached to a TSS-tag were also ligated to a PSS-tag. Indeed, in vivo, 5' triphosphate RNA ends are enzymatically converted to monophosphate, often as a first step of RNA degradation (Bail and Kiledjian 2009, and references therein). Therefore, a fraction of TSSs are expected to be associated with the PSS-tag. This effect may be further strengthened by spontaneous hydrolysis of 5' triphosphate RNA ends during the ligation step of the PSS-adaptor and preceding RNA treatments, generating 5' ends opened for ligation. On the other hand, the first step of the tagging procedure using the T4 RNA ligase is certainly not complete and acts with different efficiency on different RNA molecules (Zhuang et al. 2012; Raabe et al. 2014). Therefore, at the second ligation step, 5' monophosphate ends (i.e., PSSs) that have escaped the first tag can be ligated to the TSS-adaptor and appear as false TSSs. For each 5' RNA end mapped in this study, Figure 2A presents the number of each tag counted. The distribution of 5' termini extends continuously between the two axes and hence does not give an immediate way to distinguish TSSs from PSSs. However, the distribution can be sorted by additional arguments, paying the price of discarding information on a fraction of mapped positions. (1) PSSs (i.e., 5' monophosphate groups) for which the first ligation step was partial and also tagged with the TSS-tag sequence at the second step, should not give more TSS-tag counts than

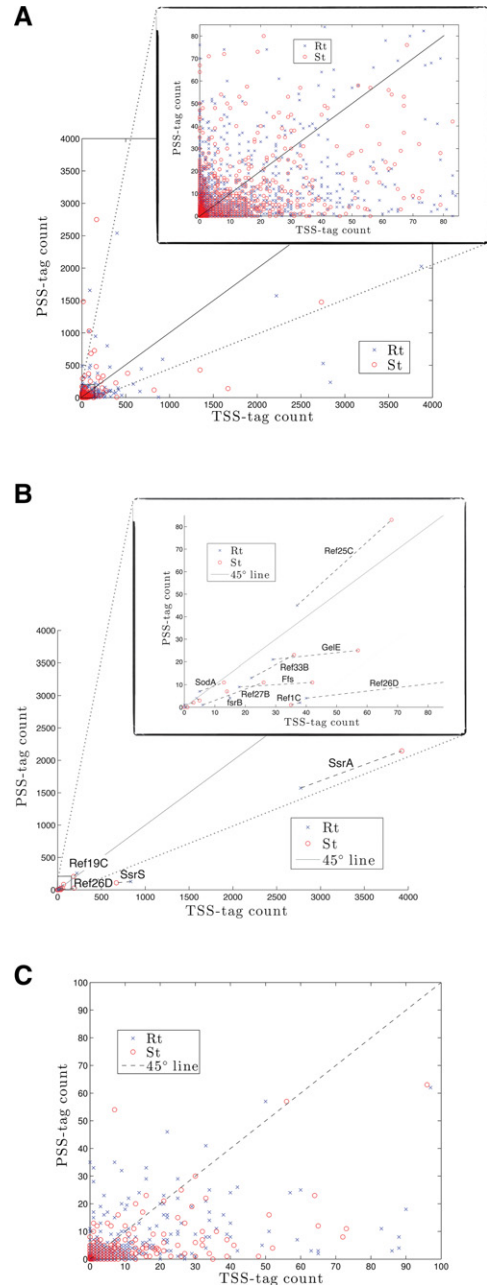


FIGURE 2. Scatter plot showing TSS-tag counts versus PSS-tag counts. (A) At each position of the genome. (B) At genomic locations within 2 bp of previously experimentally mapped transcription start sites. (C) At genomic locations within 2 bp of 5' RNA edges of transcribed regions (see Materials and Methods; Supplemental Section S3). About 80% of predicted 5' RNA ends fall below the diagonal.

PSS-tag counts since the enzyme should act with the same efficiency on the same RNA end at each step. Therefore, points (i.e., 5' RNA ends) above the diagonal may be either TSSs or partially ligated PSSs, but 5' RNA termini falling below the diagonal in Figure 2A should be TSSs. Obviously, such a cut-off eliminates true TSSs that would exist in vivo mainly as 5' monophosphate ends. (2) In accordance with the previous

argument, all other TSSs known from the literature fall below the diagonal with one exception (Fig. 2B), the ncRNA Ref25C (RNA in *E. faecalis* 25C), which we discuss in more detail in Supplemental Section S4. (3) We considered separately 5' edges of transcribed regions that feature an absence of detectable expression upstream and should therefore be a signature of a TSS. As expected for those selected RNA ends, and in accordance with the two first arguments, a clear distribution below the diagonal appears (Fig. 2C). (4) A motif search in DNA regions between 0–30 and 20–40 nt upstream of 5' RNA ends located below the diagonal shows that >80% of them contain at least one canonical sequence featuring a promoter region (–10 and/or –35 boxes). In contrast, the same search performed for 5' RNA ends above the diagonal does not retrieve any sequence reminiscent of a canonical promoter region (see below). The presence of promoter motifs in one area delineated by the diagonal is a very strong argument in favor of the location of true TSSs <45° in the plot presented in Figure 2A. Considering these rules and in order to err on the side of caution, in this work we will only consider points (i.e., 5' RNA ends) below 30° as “TSSs,” and >60° as “PSSs”; for points in between, 5' RNA ends cannot be assigned with certainty and will be considered as undetermined. Compared with other single nucleotide resolution RNA-seq methods, tagRNA-seq provides, for the first time, an accurate mapping of TSSs buried in transcribed regions and of RNA cleavage sites at a comprehensive scale in a single view, without requiring comparison between transcriptomes (Sharma et al. 2010; Nicolas et al. 2012; Wurtzel et al. 2012) (Fig. 1; the “ppRNome” browser; Supplemental Table SA).

Transcription start sites in *E. faecalis*

Within the area <30° in Figure 2A, we mapped a total of 559 TSSs on the V583 *E. faecalis* genome, combining both St and Rt (Supplemental Table SA,SB). A total of 327 TSSs were common to both transcriptomes. Among candidates classified as TSSs in St but not in Rt, 49 were classified as inconclusive due to a location between the 30° and 60° lines in Figure 2A, 1 was classified as PSS and 27 were inconclusive due to a weak (TSS-tag + PSS-tag) signal (i.e., <3.2× per million of tagged reads aligned). For the corresponding candidates in the Rt conditions, those numbers are respectively, 36 between the 30° and 60° lines, 3 classified as PSSs and 116 were inconclusive due to low signal in St (Table 1).

Motif detection and promoter features in the *E. faecalis* genome

Up to date, <50 TSSs have been experimentally characterized in *E. faecalis* (Fouquier d'Hérouël et al. 2011, and references therein). In order to better define promoter regions in this species, we took advantage of our 5' ends mapping and performed a blind search for common sequences nested in DNA regions preceding RNA extremities using the MEME suite

TABLE 1. Summary of the numbers of TSSs reported in R and S conditions

Transcriptome	St	Rt
Total TSSs detected in both conditions	559	
TSSs common across conditions	327	
Total TSSs in condition	404	482
Inconclusive due to weak signal	27	116
Inconclusive due to angle criterion	49	36
Classified as PSS	1	3
Total not classified as TSS in condition	77	155

(Bailey et al. 2009). By doing so, this search also enabled us to challenge our classification of 5' RNA ends based on the tagging method as presented in Figure 2A. We defined four groups of DNA regions: two groups below the diagonal, one from 0° to 30° (called as TSSs), a second from 30° to 45° (called as undetermined, but expected to contain mainly TSSs), and two groups above the diagonal, one from 45° to 60° (called as undetermined but with a few TSSs, e.g., Ref25C) (see Supplemental Section S4), and a second group from 60° to 90° (called as PSSs). DNA sequences used as input for MEME and a detailed list of the motifs discovered are presented in Supplemental Table SC. For groups below 30°, the analysis reveals motifs with strong statistical significance (*E*-values below 10^{-30}) and consensus sequences: Within the region [–30 ... 0] and centered around position -9.7 ± 2.6 , we found GnTATAAT, the canonical –10 box; in the [–40 ... –20] region, the motif TTGACAA was found centered at -31.5 ± 2.3 , the canonical –35 box. The –10 box appears with a high frequency (83.5%) and ends 5–9 bp from the 5' RNA ends mapped. The –35 box was found in 20.6% of input sequences. At least 90% of the sequences where a –35 box is detected also have a canonical –10 box. Boxes defined as –10 and –35 are spaced by a 16–22 bp long sequence. Thus, the most significant motifs discovered correspond to the canonical –10 (TATAAT) and –35 (TTGACA) sequences of promoters recognized by the vegetative RNA polymerase loaded with the transcription initiation factor SigA (RpoD, σ^A or σ^{70}) in the most studied bacteria *E. coli* and *B. subtilis* (Harley and Reynolds 1987; Helmann 1995). The presence and the location of –10 and –35 boxes on DNA regions upstream of 5' RNA ends falling in the area defined by the angle between 0° and 30° in Figure 2A, reinforces our previous conclusion that these RNA extremities are TSSs. In line with this conclusion, for features with an angle between 0° and 45°, –10 and –35 canonical boxes are still the most frequently found motif but the numbers fall to 80.8% and 14.7%, respectively, which indicates that the density of true TSSs is indeed higher for signals corresponding to a low angle in the plot ($\leq 30^\circ$). Within the two groups of sequences above 45°, the most significant motif discovered is AACG^A/TA^C/G^A/G, found in <10% of sequences. To our knowledge, this purine-rich motif does not resemble

any canonical sequence of bacterial promoter described previously. One might speculate that this sequence represents a frequent RNA motif targeted by an endoribonuclease, but further experiments will be required to confirm this hypothesis. Nonetheless, this observation reinforces our conclusion that the majority of TSSs do not locate $>45^\circ$ in Figure 2A.

In addition to SigA, three other sigma factors have been predicted in *E. faecalis* V583, SigH (Ef0049, the heat-shock factor), SigV (Ef3180, an “extracytoplasmic” factor) and SigN (Ef0782, a σ^{54} -like factor) (Paulsen et al. 2003). ORFs coding for SigH and SigV are not expressed in S and R growth conditions (Supplemental Table SD; the ppRNome browser), hence we did not expect to find TSSs whose promoter regions would carry consensus sequences recognized by either one of these factors. In contrast, the *sigN* encoding sequence is transcribed and we sought manually for the consensus sequence of SigN-dependent promoter ahead of TSSs mapped ($-24/-12$; TTGCCACNNNNNTTGCT) (Buck et al. 2000; Héchard et al. 2001; Iyer and Hancock 2012). Only six corresponding locations were found across the whole genome: upstream ORFs coding for components of phosphor-sugar transfer systems (PTS), *ef0019*, *ef1012*, *ef1017*, *ef1954*, *ef3210*, and *fabF-2* coding for an enzyme involved in fatty acid and biotin metabolism. Out of those six locations, the TSS for *ef1012* is detected and a tag signal below our selection threshold is found upstream of *ef1017*.

Processing sites in *E. faecalis*

PSS-tags are found $\sim 50\%$ more abundant than the number of total TSS-tags detected (Supplemental Table SA, Section S2). In contrast to TSS-tags that appear with a discrete distribution at 5' edges or nested within transcribed regions, PSS-tags, in addition to colocalize with TSS-tags, also tend to spread out over RNA signals. Although we cannot rule out experimental RNA breaks, such a distribution of PSS-tags is expected as they label any type of 5' monophosphate RNA ends, including processing sites, degradation products and hydrolyzed 5' triphosphate ends. To pinpoint major PSSs within the transcriptome, we only considered 5' ends located within the area delineated by the 60° angle in Figure 2A and above our acceptance threshold in both St and Rt. Ignoring rRNA and tRNA loci we mapped a total of 352 PSSs candidates (Supplemental Table SE).

Up to now, most of bacterial transcriptomic studies have focused on TSSs, RNA levels and the discovery of unannotated genes (e.g., Toledo-Arana et al. 2009; Sharma et al. 2010; Nicolas et al. 2012). In addition to these aspects, tagRNA-seq allows to visualize RNA processing sites and shows that the “processed RNA landscape” is an important part of the total transcriptome that has been less studied up to now. For example, the well-known ubiquitous sRNA RnpB, the ribozyme element of RNase P (Frank and Pace 1998), provides an illustration of the information accessible via tagRNA-seq. We previously mapped the *rnpB* TSS at location

1,121,939 in the *E. faecalis* V583 chromosome (Fouquier d’Hérouël et al. 2011), which is not detected by tagRNA-seq, most likely due to the higher amplification of the signal via the RACE-derivative method compared with the SOLiD procedure. The functional RnpB molecule, also termed M1, originates from a series of maturation processes conserved across the three domains of life that we may reasonably speculate to also operate in *E. faecalis* due to the high degree of structural and functional conservation of RnpB (Li et al. 1998; Mann et al. 2003; Griffiths-Jones et al. 2005, and references therein). TagRNA-seq data enables us to map locations 1,121,951/-53 with high tag counts corresponding to PSSs (Supplemental Tables SA, SE; the ppRNome browser). The RnpB upstream-most 5' end predicted in the Rfam database allocates a position at 1,121,944 in the chromosome (Griffiths-Jones et al. 2005), a location spaced by 4 and 7 nt from the TSS and PSS we have mapped, respectively.

Further experiments will be necessary to shed light on the details of the processed transcriptome and its complex organization. Nevertheless, to our knowledge, this is the first study mapping PSSs at a global scale in bacteria.

Transcription start sites and processing sites in *E. coli*

Unlike in *E. faecalis*, transcription start sites in *E. coli* have been extensively studied and TSSs have been mapped in genome-wide manner in at least three separate contributions: Mendoza-Vargas et al. (2009) reported TSSs for ~ 1000 ($\sim 23\%$) of the ~ 4500 ORFs in *E. coli* MG1655, Conway et al. (2014) mapped with high accuracy about 2100 promoters, and Thomason et al. (2015) detected over 14,000 TSSs using dRNA-seq.

In order to challenge the tagRNA-seq method and our analysis, we applied the same procedure for the *E. coli* transcriptome as we applied for *E. faecalis* with a significance threshold set to five reads. We were thus able to retrieve 397 TSSs in the U00096.3 reference genome (Supplemental Table SB). This lower number compared with *E. faecalis* can be explained by the smaller number of reads obtained from this sequencing experiment (see Supplemental Material, Section S2) and the 40% larger genome of *E. coli*, out of which $\sim 33\%$ (1.55 Mbp) appear to be transcribed in our experiment (coverage higher than $2\times$). Out of those 397 TSSs, 314 (79%) were found within 2 bp of a TSS reported in at least one of the three contributions described above (113 in Mendoza-Vargas et al. [2009], 218 in Conway et al. [2014], and 285 in Thomason et al. [2015]).

In contrast, relatively few RNA processing sites (PSSs) have been mapped with single nucleotide accuracy in *E. coli* in standard growth conditions. Supplemental Section S5 and Table S4 provides 16 examples of PSSs reported in the literature and how they appear in our results of *E. coli*: (i) 11 PSSs are clearly recovered and fall in the area $>60^\circ$, albeit three carry tag counts below the chosen threshold of five reads; (ii) five

PSSs reported elsewhere are found within the area called “undetermined” (Fig. 2). These examples support that the tagRNA-seq method enable us to map PSSs within the bacterial RNA landscape.

Nonannotated genes, small RNAs, and particular transcriptional organization

Up to now, transcriptomic studies in *E. faecalis* have used microarrays designed to examine expression of annotated ORFs (Aakra et al. 2005; Solheim et al. 2007; Makhzami et al. 2008; Vebo et al. 2009, 2010; Abrantes et al. 2011; Mehmeti et al. 2011; Vesic and Kristich 2013), or custom-made tiling arrays containing a limited number of intergenic regions (IGRs) to search for sRNAs (Shioya et al. 2011). Although informative, these approaches provide partial information on the bacterial transcriptome compared with RNA-seq methods (Sittka et al. 2008; Rasmussen et al. 2009; Toledo-Arana et al. 2009; Sharma et al. 2010; Chao et al. 2012; Nicolas et al. 2012). We took advantage of our 5' RNA end mapping for a detailed transcriptional analysis, looking for previously nonannotated genes in the genome of *E. faecalis* V583. Among other transcripts, sRNAs were primarily identified as stand-alone signals, whose length is up to 500 nt, located in “empty” regions (i.e., nonannotated regions), or transcripts antisense to annotated ORFs. In addition to the sRNAs previously identified (Fouquier d'Hérouël et al. 2011; Shioya et al. 2011), we unveiled a total of 85 novel sRNAs (Fig. 3; Supplemental Table SF). Continuing on our previous nomenclature (Fouquier d'Hérouël et al. 2011), these new sRNAs were named from “Ref47” to “Ref120” when present in the chromosome, and for sRNAs encoded by plasmids pTEF1 and pTEF2, from “RefA1” to “RefA9” and “RefB1” to “RefB12,” respectively. Among the 45 sRNAs previously reported in Fouquier d'Hérouël et al. (2011), 18 are confirmed by tagRNA-seq. For the remaining 27, we detect some low and inconclusive signals for about half of them, and do not detect anything for the rest. Four among the 11 unnamed sRNAs reported in Shioya et al. (2011) were confirmed and named *Ref57* (IGR *ef0408-9* in the chromosome), *Ref78* (IGR *ef1368-9*), *RefA9* (IGR *efa0080-1* in pTEF1), and *RefB12* (IGR *efb0062-63* in pTEF2) (Supplemental Table SF). Additionally, comparison with Table S3 in the supplementary material of Shioya et al. (2011) confirmed six sRNAs in our list (*Ref81*, *Ref115*, *RefA3*, *Ref93A,B*, *RefA8*, and *RefB11*), as well as the antisense to *RefA7* observed in our ex-

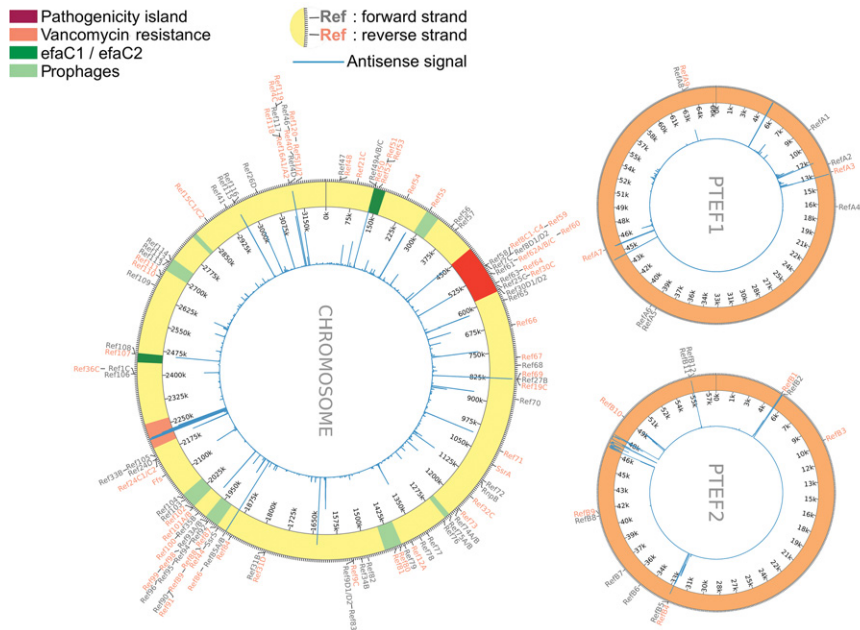


FIGURE 3. Global view of sRNAs and antisense organizations currently known in *E. faecalis* V583 (the chromosome and plasmids pTEF1 and pTEF2). All the sRNAs from Supplemental Table SF are represented, in “gray” on the forward strand and “orange” on the reverse strand. The inner plot visually describes with vertical blue lines the location and importance of antisense organizations detected (see the ppRNome browser for details). On the chromosome, the pathogenicity island (red) and other mobile genetic elements are annotated on the chromosome, i.e., *efaC1/C2* (dark green), vancomycin resistance region (orange), and the six prophages (bright green) (Lepage et al. 2006; Matos et al. 2013).

periment but unnamed due to absence of tags, and the long 3' UTR of *ef3249*.

sRNAs have important regulatory functions. Generally, regulatory RNAs not embedded in a transcriptional antisense organization (stand-alone) modulate the activity of proteins or affect translation (up or down) by pairing to mRNAs; a class of sRNAs also named “*trans-acting* sRNAs” (Repoila and Darfeuille 2009; Waters and Storz 2009). Although not functionally characterized so far, many sRNAs found in *E. faecalis* are likely *trans-acting* regulators, e.g., *Ref50*, *Ref52*, *Ref72*, *Ref78*, *Ref79*, *Ref95*, *Ref102*, *RefA1*, *RefA4* (Supplemental Table SF). Some sRNAs have been shown to carry a dual function since they can exert their regulatory role via different mechanisms or can also encode peptides (Wadler and Vanderpool 2007; Loh et al. 2009; Livny and Waldor 2010; Jørgensen et al. 2012; Sayed et al. 2012). Some of the sRNAs predicted here may also encode for peptides as previously predicted for other sRNAs in *E. faecalis* (Fouquier d'Hérouël et al. 2011). Another category of sRNAs are antisense RNAs (asRNAs), transcribed from the complementary DNA strand of genes, and thereby forming transcriptional antisense organizations. As regulatory consequence, the expression of an asRNA can potentially impact the transcription initiation efficacy of the opposite gene (promoter interference), may provoke premature arrest of transcription elongation, and/or possibly modulate the

translation and the stability of the cognate RNA (Georg and Hess 2011; Brantl 2012; Sesto et al. 2013). Many of the novel RefsRNAs appear to form antisense transcriptional organizations, e.g., Ref89 and RefB4 are antisense to sRNAs Ref90, RefB5, respectively; Ref94, Ref114, and Ref115 are antisense to transcripts bearing ORFs *ef2025*, *ef3087*, and *ef3088*, respectively (Supplemental Table SF).

Also, long 3' UTRs have been reported in several bacterial species and in a few cases their involvement in RNA-mediated regulation has been demonstrated (Sittka et al. 2008; Chao et al. 2012). In Supplemental Section S6, we present several cases found in the genome of V583.

In addition, antisense transcriptional organization also results from overlapping mRNAs and may involve coding sequences as well as 5' or 3' UTRs (e.g., Rasmussen et al. 2009; Toledo-Arana et al. 2009; Sharma et al. 2010; Nicolas et al. 2012; Wurtzel et al. 2012). For instance, the 5' UTR *ef0282* (*fabI*) overlaps the 5' UTR *ef0283* (*fab-F1*); ORFs *ef0479*, and *ef0480* are embedded in a long opposite transcript originating 3000 bp upstream; and the transcript that contains *ef0522–ef0523* in an operon is antisense to a transcript carrying *ef0524*. Similar examples are observed on plasmids pTEF1 and pTEF2 (the ppRNome browser and Supplemental Table SF). However, one of the most striking antisense organizations was found in the region spanning from *ef2298* to *ef2324* (Fig. 4). It is clearly visible in all of the *E. faecalis* transcriptomes, regardless of the growth condition, tagging, or sequencing protocol. It encompasses ~22 kbp on the chromosome and involves two transcribed regions of 16 and 17 kbp long that overlap by 11.6 kbp. In the positive direction, the transcribed RNA originates 265 bp upstream of *ef2304*, the unique predicted ORF contained within this 16 kbp long RNA, and would code for a putative transcriptional regulator (Paulsen et al. 2003). In addition, this RNA is

antisense to *ef2312* and *ef2314* that code for the DNA topoisomerase III (TopB-2) and a putative bacteriocin, respectively. On the negative strand, the second RNA originates 225 bp upstream of *ef2308*, and carries *ef2298* and *ef2299* (Fig. 4). These later ORFs encode the two-component regulatory system VanRB/SB, a vital element for *E. faecalis* V583 to resist to vancomycin, a major clinical antibiotic against Gram-positive infections (Huycke et al. 1998; Arias and Murray 2012). Experimental validation will be required, but it is tempting to speculate that this antisense regulation may control vancomycin resistance in *E. faecalis* V583.

Differential gene expression in static and respiratory growth

We performed a standard differential expression analysis between the R and S conditions for *E. faecalis* (see Materials and Methods; Supplemental Table SD). Annotation and gene ontology information show that most of the differentially expressed genes in Supplemental Table SD are involved in the central metabolism associated with the consumption of sugars and amino acids as sources of carbon and nitrogen, mainly centered on glycolysis, pyruvate metabolism, and citrate cycle (TCA) (<http://www.genome.jp/kegg/pathway.html> and Fig. 5). For instance, operons *celAB*, *ef1017–ef1020*, and *ef2959–ef2961* have a higher expression in S compared with R conditions, and are predicted to code for phosphor-sugar transfer systems (PTSs) of cellobiose and ribose uptake, and degrading enzymes, respectively. These transporter systems allow the entry and the phosphorylation of specific sugars that are catabolized via the glycolytic pathway. In R, compared with S conditions, an increased expression is detected for operons *ef0097–ef0100* that code for the subunits

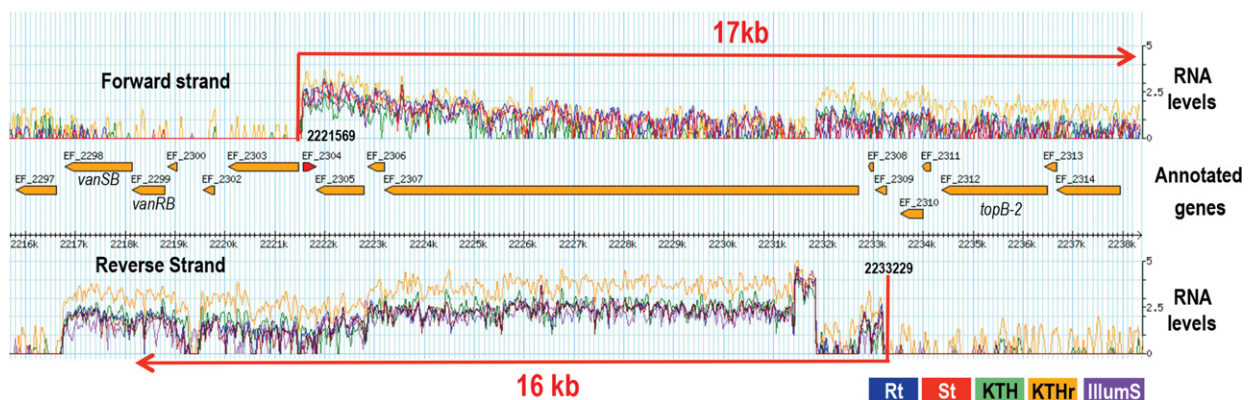


FIGURE 4. Long antisense organization in the chromosome of *E. faecalis* V583. The transcriptional antisense organization encompasses 22 kbp. Note that only a single ORF, *ef2304*, is predicted in the transcript originated from the positive DNA strand at coordinate 2221569. ORFs, *ef2312* and *ef2314* encode the DNA topoisomerase III and a putative bacteriocin; they are not transcribed in the growth conditions used but are “covered” by the antisense RNA (17 kb). *vanRB* and *vanSB*, encoding the two-component regulatory system of the vancomycin resistance locus, are contained at the end of the transcript originated at coordinate 2233229 from the minus DNA strand. The two antisense RNAs overlap by 11.6 kb. Coordinates mapped for TSSs of each corresponding transcript are noted at the corresponding location. The color boxes denoted by “Rt,” “St,” “KTH,” “KTHr,” and “IlluminaSt” applied to RNA levels of corresponding transcriptomes. RNA levels shown are normalized.

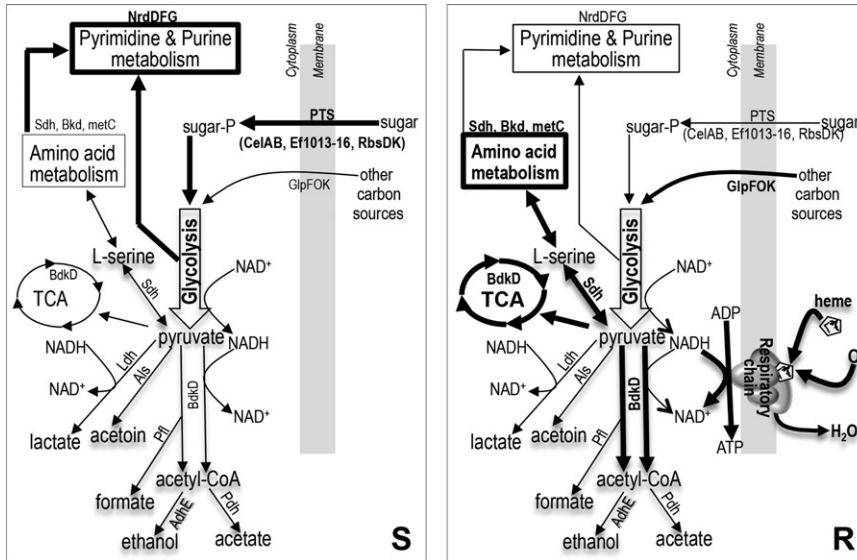


FIGURE 5. Metabolic pathways deduced from functions assigned to RNAs differentially expressed in S and R growth conditions. Transcriptomes St and Rt both show significant expression of genes involved in central metabolism. Differential expression analysis indicates that groups of enzymes specifically involved in sugar uptake systems (PTSs) and nucleotide bases metabolism pathways are induced in static growth conditions (S). Similarly, in respiration (R), the formation of acetyl-CoA from pyruvate, formate, and ethanol is enhanced, as well as the citrate cycle (TCA) and amino acids metabolism. Genes with up-regulated expression in each condition are represented by thick arrows in the corresponding plot. The names on the arrows correspond to gene names as given in Supplemental Table SD, which also contains their assigned functions from the KEGG database.

of the serine-dehydratase (Sdh) that converts serine into pyruvate (or the reverse reaction), the end product of glycolysis, and *ef1657–ef1663* coding for enzymes that feed or make part of the TCA cycle and glycolysis, and participate to amino acid metabolism (valine and serine) from pyruvate. We also observed an increased expression in R for operon *glpFOK* (*ef1927–ef1929*) coding for enzymes enabling glycerol catabolism via glycolysis in aerobic conditions (Bizzini et al. 2010).

The results of this standard differential expression analysis are in line with previous reports on metabolic and transcriptomic studies performed on *E. faecalis* and closely related species such as *Lactococcus lactis* (Garrigues et al. 1997; Redon et al. 2005; Pedersen et al. 2008). Under S conditions (anaerobic growth) and, in the growth medium used in this study, *E. faecalis* adopts fermentation, a physiological state characterized by a high rate of sugar consumption in comparison to respiration, and employs the glycolysis pathway for glucose catabolism, ending up in pyruvate formation (Garrigues et al. 1997; Pfeiffer et al. 2001). In *E. faecalis*, the respiratory chain is complete but not functional as genes encoding enzymes required for heme synthesis are absent. However, if oxygen and heme are supplied as in R growth conditions, *E. faecalis* switches from homolactic fermentation to respiration and under respiration, pyruvate conversion is not exclusively catalyzed by Ldh-1, but also by Als (Ef1213), Pdh (Ef1353/Ef1354), Pfl (Ef1612/Ef1613), and AdhE (Ef0900), ending in the production of various products (acetate, etha-

nol, formate), and regenerate NAD⁺ from NADH (Winstedt et al. 2000; Yamamoto et al. 2006; Pedersen et al. 2008).

In summary, with the caveats of high expected false negative rate when comparing few samples, it can be checked that all the reported variations in Figure 5 and Supplemental Table SD are consistent with previously reported features of *E. faecalis* biology with and without respiration.

CONCLUSION

In this work, we have introduced a new method to distinguish primary and processed RNA ends and achieved the first RNA-seq transcriptome of *E. faecalis*. The discovery of numerous sRNAs and antisense organizations in *E. faecalis* transcriptomes highlights, as in many other species, the importance of RNA-dependent regulatory processes. The association of the RNA-seq method with the differential labeling of 5' RNA ends, enabled us to provide the two “faces” of a bacterial RNA landscape. We mapped 559 TSSs and predicted promoter motifs

at the genome-wide scale in a species where <50 were previously known, and 352 major PSSs, providing a first snapshot of a bacterial processed RNA landscape. As TSS- and PSS-tags hallmark transcription initiation and processing, the next step in the exploitation of our technology allowing identification of 5' ends of primary and processed transcripts will be to perform quantitative studies in order to pinpoint the contribution of RNA synthesis and RNA stability in gene expression reprogramming accompanying physiological adaptation. This study constitutes a significant advance in the understanding of the organization and the expression of the genetic information of the human pathogen *E. faecalis*, and a key improvement of the functional analysis of bacterial transcriptomes.

MATERIALS AND METHODS

Bacterial growth and RNA preparation

E. faecalis V583 (VE14002 in our laboratory collection) was grown in brain–heart infusion (BHI) medium at 37°C in static (S) or respiratory (R) conditions. Briefly, one fresh bacterial colony was used to inoculate 5 mL BHI and grown at 37°C in S conditions for 20 h. A 1/500 dilution was then made in prewarmed BHI medium to obtain the test culture. In S growth conditions, the culture was not shaken. In R growth, hemin (SIGMA) was added to the test culture at 10 μM final concentration and culture was shaken at 200 rpm. Bacterial

growth was followed by measuring the optical density at 600 nm (OD600). Total RNAs were prepared from bacterial cultures grown to an optical density (OD600) ranging between 0.7 and 0.85, as previously described (Fouquier d'Hérouël et al. 2011). In the course of this work, we discovered that our laboratory strain did not contain the plasmid pTEF3 (Paulsen et al. 2003); although we used the appellation of “V583” throughout the text, data presented are those obtained for our strain VE14002.

E. coli strain MG1655 was grown in LB medium at 37°C under agitation (200 rpm) until an OD600 of 0.5. Bacteria were pelleted and total RNA prepared as previously described (Fouquier d'Hérouël et al. 2011).

RNA tagging and sequencing

In bacteria, transcriptional start sites (TSSs, or “+1”) are characterized by the presence of a 5' triphosphate group. In contrast, 5' RNA ends created by endonucleolytic cleavages (PSSs) are 5' monophosphate. We exploit this chemical difference by labeling differentially mono- and triphosphate 5' RNA ends with two short RNA oligonucleotides, the “tags” (Fouquier d'Hérouël et al. 2011).

5' RNA ends were differentially labeled with two short and different RNA oligonucleotides (tags) (Fouquier d'Hérouël et al. 2011; Supplemental Section S1). Briefly, primary transcripts contain 5' ends with a triphosphate group which is brought by the first nucleotide triphosphate used by the RNA polymerase to initiate RNA synthesis at TSSs. In contrast, RNA processing events generate, at cleavage sites (PSSs), 5' ends with monophosphate groups. RNAs with PSS and hydrolyzed 5' triphosphate RNA ends were tagged by a first ligation step with the PSS-RNA adaptor (PSS-tag). Subsequently, RNAs were treated with the tobacco alkaline phosphatase (TAP) to transform triphosphate groups into monophosphate groups and were then tagged by a second ligation step with a TSS-RNA adaptor (TSS-tag). TSS- and PSS-tag sequences were adapted to RNA-seq in such a way that they cannot be mistaken with any regions of the V583 reference genome (Supplemental Section S1).

In order to account for variations in total number of reads and to be able to compare experiments, RNA levels are reported normalized to the total number of reads mapped, as commonly done in RNA-seq (Robinson and Oshlack 2010). Additionally, the ligation procedure introduces a new variability in the experiment that is corrected for by normalizing the number of tagged reads mapped at a given position to the total number of tagged reads mapped for the entire V583 genome (Supplemental Table SA).

Two RNA libraries were obtained from total RNAs prepared from *E. faecalis* grown in S and R conditions. They were tagged with PSS- and TSS-tags according to our 5' RNA end discriminative method, treated according to SOLiD manufacturer's protocols for sequencing (Applied Biosystems, Life Technologies Corporation), and sequenced on a SOLiD 5500 platform (MetaGenoPolis, INRA). The corresponding transcriptomes were named “St” and “Rt,” respectively (Supplemental Table SA).

Additionally, as control, three other RNA libraries prepared from two independent growths in S conditions were sequenced. In one experiment, the bacterial culture was grown at Karolinska Institute, Sweden, as previously described in Fouquier d'Hérouël et al. (2011), and sequenced on a SOLiD v3 platform (Viiki) without applying our tagging procedure. Two libraries, denoted as “KTHr”

and “KTH” respectively, were prepared from this experiment. For one of them, ribosomal RNAs (rRNAs) were removed using Ambion MICROBExpress Bacterial mRNA Enrichment Kit; in the other, rRNAs were retained. In the second S growth culture, bacteria were grown at INRA and RNAs were prepared as described here. Sequencing was done on a Hi-seq platform (IMAGiF, CNRS) following the Illumina TruSeq protocol, resulting in the “IlluminaSt” transcriptome. Due to technicalities in the ligation, the tagging in this sample was ineffective leading to a sample that here has been used only as standard RNA-seq.

A single RNA sample was prepared from *E. coli* total RNA, tagged using the same RNA adaptors (TSS- and PSS-tags) and sequenced on the SOLiD Wildfire platform (MetaGenoPolis, INRA). The resulting transcriptome was named “Coli.”

Alignment and coverage

Reads were aligned to the *E. faecalis* v583 and *E. coli* K12 substrain MG1655 reference genomes (respectively, GenBank Accession IDs [GenBank:AE016830.1] (chromosome), [GenBank:AE016831.1] (pTEF2), and [GenBank:AE016833.1] (pTEF1); [GenBank:U00096.3]) using Bowtie 1.0.0 (Langmead et al. 2009) with default options, but allowing for multiple matches (-a best command line option). The coverage is calculated by counting the number of reads mapped at each position on the genome for each strand. In case of multiple matches, the number of matches correspondingly divides the contribution to the read count. In cases mentioned explicitly in the text where repeated regions are excluded from the analysis; those multiply matched reads are ignored in the count. Similarly, when rRNAs and tRNAs are excluded, we impose a zero coverage over the corresponding regions. In order to reduce the effect of fragment bias (reads that are not uniformly distributed within the transcripts they represent) (Roberts et al. 2011), we define a quantity called “coverage density” similar to the coverage, except that reads mapped so that they start at the same genomic position are counted only once. The resulting signal is thus less sensitive to the specific amplification of the different fragments at the cost of losing dynamic range. The coverage density signal has the useful and exploitable feature that edges of an expressed region are always staircase-shaped. We use the coverage density signal as a means to predict transcript edges from our RNA-seq data. Supplemental Section S2 compiles the raw sequencing output for the various transcriptomes performed.

Gene expression level

We calculated gene expression levels of annotated genes of the *E. faecalis* genome and performed differential expression analysis between R and S growth condition using Cuffdiff from the Cufflinks suite v2.1.1 (Trapnell et al. 2010). Cuffdiff was run on the Bowtie output files with the command line option -u -library-type fr-secondstrand using the genome of *E. faecalis* V583 and its annotation. Regions corresponding to rRNA in the annotation were masked using the -M option.

Comparing Rt and St, we obtained a list of 31 ORFs that displayed significant variation of RNA levels between the two tagged RNA-seq (Supplemental Table SD). We assessed the false positive rate by comparing to the results including in the analysis data from the “IlluminaSt” transcriptome in the S growth condition. This

improves the prediction quality of some called genes (decreases P -values for 16 ORFs), adds 16 more called genes to the list (moves their P -values below threshold), and still calls 23 ORFs in the list. For the nine ORFs that are removed from the list, the P -value, on the other hand, increases above threshold. Results from the analysis are available in Supplemental Table SD and discussed in the Results and Discussion section.

Predictions of transcription start sites

Starting from the coverage density signal, we developed an iterative algorithm to detect transcribed regions, filtering out signals of low quality originating from sequencing errors or misalignments. The algorithm is inspired by the edge thinning operation in image processing (Davies and Plummer 1981). All regions where the signal is greater than a given but arbitrary confidence threshold are marked as “strong” signal. The signal in the immediate vicinity of this strong signal is recursively annexed to the strong signal region. All signals not marked as strong are discarded (Supplemental Section S3). The algorithm discriminates low signals within transcribed regions and eliminates those likely caused by noise. The orientation of the aligned reads and the edges of signals enable us to assign TSSs.

Detection of transcription starts and processing sites using 5' tags

The addition of tags allows to readily map 5' ends of RNA molecules and to discriminate primary transcripts (ligated to TSS-tags) from processed transcripts (ligated to PSS-tags). Prior to alignment, reads are sorted according to tag sequences or their absence and, when present, tag sequences are removed from reads, leaving only sequences from bacterial RNAs. Both operations are performed simultaneously with Flexbar—Flexible Barcode and adapter removal for sequencing platforms—v2.4 (Dodt et al. 2012) allowing for up to two mismatches in the 13 nt of the tags (command line parameters `-barcode-trim-end LEFT -barcode-threshold 1.6 -barcode-unassigned -barcode-min-overlap 9 -min-read-length 35`). After alignment, reads with tags are classified into TSS or PSS candidates according to the rules described in the Results and Discussion section “The calling of TSS and PSS from tagRNA-seq.”

For transcriptomes obtained from the Illumina Hi-seq and SOLiD Wildfire, standard removal of 3' sequencing adapters is performed using Flexbar in an additional preprocessing step. This step is not needed for SOLiD v3 and 5500 where the insert size is typically much longer than read length (Innocenti and Aurell 2013).

As a 5' RNA end can be tagged by both TSS-tag and PSS-tag sequences (see below), we considered a 5' end to be present in the sequenced RNA population when at a given location, the sum of TSS-tags and PSS-tags have counts of at least $3.2\times$ per million of tagged reads aligned in *E. faecalis* transcriptomes. Such a threshold corresponds to a total of 5 tags (TSS- + PSS-tags) detected at the concerned position for the St transcriptome and seven tags for Rt. For the “Coli” transcriptome, this threshold was kept at 5 tags, or $4.06\times$ per million of tagged reads aligned.

On one hand, a careful examination of the transcriptomes reveals many instances of one or two isolated reads in isolated positions. It is reasonable to assume that many of these are noise and thus setting the limit above this level was chosen to eliminate them. On the other

hand, as described in detail in Supplemental Section S7, there seems to be no natural threshold in the data and a lower threshold simply leads to more candidates. The threshold values given above are simply one reasonable choice.

It is well known that transcription initiation at a transcription start site is not always initiated with single nucleotide accuracy (Schlüter et al. 2010; Sharma et al. 2010; Cortes et al. 2013; Morton et al. 2014). To take this into account, when locations distant by 4 bp or less from each other have mapped reads with TSS-tags and at least one of them is classified as a TSS candidate, the multiple tag signals are grouped in a single region that encompasses all those locations (Supplemental Tables SA, SB). The location with the highest tag signal is taken to be the most probable location of the TSS, and the total tag signal for the region is taken as the sum of the signals at all locations in the group. Although the length of such a “TSS region” can reach 6 bp or more in rare cases, many TSSs are detected with single nucleotide resolution (Supplemental Figs S8a,b in Section S8). Furthermore, an analysis of the average signal around retrieved TSSs shows that most of the signal concentrates within a region of ± 2 bp around the most probable location (Supplemental Fig. S8c in Section S8).

As much less is known about the accuracy of the different ribonucleases, PSSs are reported in the text as point location on the genome and neighboring nucleotides with tag signal classified as PSSs are counted as different PSS sites.

Motif detection

We performed unbiased de novo motif search using MEME v4.9.1 (Bailey et al. 2009) upstream of genomic positions with TSSs and PSSs. The search was limited to the 10 most significant motifs with a width between 4 and 8 bp (command line arguments `-nmotifs 10 -minw 4 -maxw 8`). Short DNA sequences were extracted from the reference genome between [20–40 bp] and [0–30 bp] upstream of locations of interest and classified according to their ratios of PSS to TSS tag signals (as described in the Results and Discussion section “The calling of TSS and PSS from tagRNA-seq”). Those sequences were used as input to MEME without any filtering. When the feature was a TSS region as defined in the previous section, the most probable location was used as reference position for the sequence. The list of input sequences and results of the analysis are available Supplemental Table SC.

Visualization of results

All coverage information and tag signals resulting from our experiments and analysis can be visualized in a user-friendly and interactive manner online at the address http://ebio.u-psud.fr/eBIO_BDD.php (select the entry called “The ppRNome browser”). The visualization uses the Genome Browser (GBrowse) (Supplemental Section S9; Stein et al. 2002). The data presented online are also available in a numerical format in Supplemental Tables SA and SD for the Rt and St transcriptomes.

DATA DEPOSITION

The data are available in NCBI SRA repository, reference number PRJNA272574.

SUPPLEMENTAL MATERIAL

Supplemental material is available for this article.

ACKNOWLEDGMENTS

We thank the eBIO computing platform of Orsay, particularly C. Drevet and C. Toffano-Nioche, for hosting the “ppRNome browser.” We thank Ingemar Ernberg at Karolinska Institutet for his hospitality by providing laboratory space and equipment for A. F.d’H., and V. Cantoni for the suggestion to use edge detection algorithms. We are grateful to the “CPE team,” A. Gruss, and D. Halpern for comments and discussions, and to S. Gaubert, L. Girbal, T. Esquerré, and M. Coccagn-Bousquet for communicating results prior to publication. Many thanks to our colleagues, P. Palcy, V. Bourgoigne, N. Eberlin, and P. Régent for invaluable administrative, IT, and equipment-related support. This research was supported by the Swedish Science Council through grant 621-2012-2982 (E.A.), and by the Academy of Finland through Finland Distinguished Professor Programme and the Center of Excellence COIN (E.A.), and grant ANR-12-BSV6-0008 (ReadRNA) from the Agence Nationale pour la Recherche.

Authors’ contributions: N.I., A.F.d’H., F.R., and E.A. designed the research. N.I., M.G., A.F.d’H., and E.A. developed and performed the computational analysis and visualization on website. A.F.d’H., C.L., R.A.B., F.W., P.S., and F.R. performed bacterial manipulation, RNA extractions, and tagRNA libraries preparation. S.P.K. performed the SOLiD tagRNA sequencing. N.I., A.F.d’H., P.S., P.B., F.R., and E.A. analyzed data and wrote the paper. All authors read and approved the final manuscript.

Received October 7, 2014; accepted December 22, 2014.

REFERENCES

- Aakra Å, Vebø H, Snipen L, Hirt H, Aastveit A, Kapur V, Dunny G, Murray BE, Nes IF. 2005. Transcriptional response of *Enterococcus faecalis* v583 to erythromycin. *Antimicrob Agents Chemother* **49**: 2246–2259.
- Aakra Å, Vebø H, Indahl U, Snipen L, Gjerstad Ø, Lunde M, Nes IF. 2010. The response of *Enterococcus faecalis* v583 to chloramphenicol treatment. *Int J Microbiol* **2010**: 483048.
- Abrantes MC, Lopes Mde F, Kok J. 2011. Impact of manganese, copper and zinc ions on the transcriptome of the nosocomial pathogen *Enterococcus faecalis* v583. *PLoS One* **6**: e26519.
- Alderberth I, Wold AE. 2009. Establishment of the gut microbiota in Western infants. *Acta Paediatr* **98**: 229–238.
- Albrecht M, Sharma CM, Reinhardt R, Vogel J, Rudel T. 2010. Deep sequencing-based discovery of the *Chlamydia trachomatis* transcriptome. *Nucleic Acids Res* **38**: 868–877.
- Arias CA, Murray BE. 2012. The rise of the *Enterococcus*: beyond vancomycin resistance. *Nat Rev Microbiol* **10**: 266–278.
- Bail S, Kiledjian M. 2009. Tri- to be mono- for bacterial mRNA decay. *Structure* **17**: 317–319.
- Bailey TL, Boden M, Buske FA, Frith M, Grant CE, Clementi L, Ren J, Li WW, Noble WS. 2009. MEME Suite: tools for motif discovery and searching. *Nucleic Acids Res* **37**: W202–W208.
- Bizzini A, Zhao C, Budin-Verneuil A, Sauvageot N, Giard JC, Auffray Y, Hartke A. 2010. Glycerol is metabolized in a complex and strain-dependent manner in *Enterococcus faecalis*. *J Bacteriol* **192**: 779–785.
- Bohn C, Rigoulay C, Chabelskaya S, Sharma CM, Marchais A, Skorski P, Borezée-Durant E, Barbet R, Jacquet E, Jacq A, et al. 2010. Experimental discovery of small RNAs in *Staphylococcus aureus* reveals a riboregulator of central metabolism. *Nucleic Acids Res* **38**: 6620–6636.
- Brantl S. 2012. Acting antisense: plasmid- and chromosome-encoded sRNAs from Gram-positive bacteria. *Future Microbiol* **7**: 853–871.
- Buck M, Gallegos MT, Studholme DJ, Guo Y, Gralla JD. 2000. The bacterial enhancer-dependent σ^{54} (σ^N) transcription factor. *J Bacteriol* **182**: 4129–4136.
- Campeotto F, Waligora-Dupriet AJ, Doucet-Populaire F, Kalach N, Dupont C, Butel MJ. 2007. Establishment of the intestinal microflora in neonates. *Gastroenterol Clin Biol* **31**: 533–542.
- Chao Y, Papenfort K, Reinhardt R, Sharma CM, Vogel J. 2012. An atlas of Hfq-bound transcripts reveals 3’ UTRs as a genomic reservoir of regulatory small RNAs. *EMBO J* **31**: 4005–4019.
- Conway T, Creecy JP, Maddox SM, Grissom JE, Conkle TL, Shadid TM, Teramoto J, San Miguel P, Shimada T, Ishihama A, et al. 2014. Unprecedented high-resolution view of bacterial operon architecture revealed by RNA sequencing. *MBio* **5**: e01442–e01414.
- Cortes T, Schubert OT, Rose G, Arnvig KB, Comas I, Aebersold R, Young DB. 2013. Genome-wide mapping of transcriptional start sites defines an extensive leaderless transcriptome in *Mycobacterium tuberculosis*. *Cell Rep* **5**: 1121–1131.
- Davies ER, Plummer APN. 1981. Thinning algorithms: a critique and a new methodology. *Pattern Recognit* **14**: 53–63.
- Dot M, Roehr JT, Ahmed R, Dieterich C. 2012. FLEXBAR—flexible barcode and adapter processing for next-generation sequencing platforms. *Biology* **1**: 895–905.
- Esquerré T, Laguerre S, Turlan C, Carpousis AJ, Girbal L, Coccagn-Bousquet M. 2013. Dual role of transcription and transcript stability in the regulation of gene expression in *Escherichia coli* cells cultured on glucose at different growth rates. *Nucleic Acids Res* **42**: 2460–2472.
- Fouquier d’Hérouël A, Wessner F, Halpern D, Ly-Vu J, Kennedy SP, Serron P, Aurell E, Repoila F. 2011. A simple and efficient method to search for selected primary transcripts: non-coding and antisense RNAs in the human pathogen *Enterococcus faecalis*. *Nucleic Acids Res* **39**: e46.
- Frank DN, Pace NR. 1998. Ribonuclease P: unity and diversity in a tRNA processing ribozyme. *Annu Rev Biochem* **67**: 153–180.
- Garrigues C, Loubiere P, Lindley ND, Coccagn-Bousquet M. 1997. Control of the shift from homolactic acid to mixed-acid fermentation in *Lactococcus lactis*: predominant role of the NADH/NAD⁺ ratio. *J Bacteriol* **179**: 5282–5287.
- Georg J, Hess WR. 2011. cis-antisense RNA, another level of gene regulation in bacteria. *Microbiol Mol Biol Rev* **75**: 286–300.
- Gilmore MS, Ferretti JJ. 2003. Microbiology. The thin line between gut commensal and pathogen. *Science* **299**: 1999–2002.
- Griffiths-Jones S, Moxon S, Marshall M, Khanna A, Eddy SR, Bateman A. 2005. Rfam: annotating non-coding RNAs in complete genomes. *Nucleic Acids Res* **33**: D121–D124.
- Hambraeus G, von Wachenfeldt C, Hederstedt L. 2003. Genome-wide survey of mRNA half-lives in *Bacillus subtilis* identifies extremely stable mRNAs. *Mol Genet Genomics* **269**: 706–714.
- Harley CB, Reynolds RP. 1987. Analysis of *E. coli* promoter sequences. *Nucleic Acids Res* **15**: 2343–2361.
- Hécharde Y, Pelletier C, Cenatiempo Y, Frère J. 2001. Analysis of σ^{54} -dependent genes in *Enterococcus faecalis*: A mannose PTS permease (EII^{Man}) is involved in sensitivity to a bacteriocin, mesentericin Y105. *Microbiology* **147**: 1575–1580.
- Helmann JD. 1995. Compilation and analysis of *Bacillus subtilis* σ^A -dependent promoter sequences: evidence for extended contact between RNA polymerase and upstream promoter DNA. *Nucleic Acids Res* **23**: 2351–2360.
- Huycke MM, Sahn DF, Gilmore MS. 1998. Multiple-drug resistant enterococci: the nature of the problem and an agenda for the future. *Emerg Infect Dis* **4**: 239–249.
- Innocenti N, Aurell E. 2013. Lognormality and oscillations in the coverage of high-throughput transcriptomic data towards gene ends. *J Stat Mech* P10013.

- Irnov I, Sharma CM, Vogel J, Winkler WC. 2010. Identification of regulatory RNAs in *Bacillus subtilis*. *Nucleic Acids Res* **38**: 6637–6651.
- Iyer VS, Hancock LE. 2012. Deletion of σ^{54} (rpoN) alters the rate of autolysis and biofilm formation in *Enterococcus faecalis*. *J Bacteriol* **194**: 368–375.
- Jørgensen MG, Nielsen JS, Boysen A, Franch T, Møller-Jensen J, Valentin-Hansen P. 2012. Small regulatory RNAs control the multi-cellular adhesive lifestyle of *Escherichia coli*. *Mol Microbiol* **84**: 36–50.
- Kristoffersen SM, Haase C, Weil MR, Passalacqua KD, Niazi F, Hutchison SK, Desany B, Kolstø AB, Tourasse NJ, Read TD, et al. 2012. Global mRNA decay analysis at single nucleotide resolution reveals segmental and positional degradation patterns in a Gram-positive bacterium. *Genome Biol* **13**: R30.
- Langmead B, Trapnell C, Pop M, Salzberg SL. 2009. Ultrafast and memory-efficient alignment of short DNA sequences to the human genome. *Genome Biol* **10**: R25.
- Lepage E, Brinster S, Caron C, Ducroix-Crepy C, Rigottier-Gois L, Dunny G, Hennequet-Antier C, Serror P. 2006. Comparative genomic hybridization analysis of *Enterococcus faecalis*: identification of genes absent from food strains. *J Bacteriol* **188**: 6858–6868.
- Li Z, Pandit S, Deutscher MP. 1998. 3' Exoribonucleolytic trimming is a common feature of the maturation of small, stable RNAs in *Escherichia coli*. *Proc Natl Acad Sci* **95**: 2856–2861.
- Livny J, Waldor MK. 2010. Mining regulatory 5'UTRs from cDNA deep sequencing datasets. *Nucleic Acids Res* **38**: 1504–1514.
- Loh E, Dussurget O, Gripenland J, Vaitkevicius K, Tiensuu T, Mandin P, Repoila F, Buchrieser C, Cossart P, Johansson J. 2009. A trans-acting riboswitch controls expression of the virulence regulator PrfA in *Listeria monocytogenes*. *Cell* **139**: 770–779.
- Makhzami S, Quéneé P, Akary E, Bach C, Aigle M, Delacroix-Buchet A, Ogier JC, Serror P. 2008. In situ gene expression in cheese matrices: application to a set of enterococcal genes. *J Microbiol Methods* **75**: 485–490.
- Mann H, Ben-Asouli Y, Schein A, Moussa S, Jarrous N. 2003. Eukaryotic RNase P: role of RNA and protein subunits of a primordial catalytic ribonucleoprotein in RNA-based catalysis. *Mol Cell* **12**: 925–935.
- Matos RC, Lapaque N, Rigottier-Gois L, Debarbieux L, Meylheuc T, Gonzalez-Zorn B, Repoila F, Lopes Mde F, Serror P. 2013. *Enterococcus faecalis* prophage dynamics and contributions to pathogenic traits. *PLoS Genet* **9**: e1003539.
- Mehmeti I, Jönsson M, Fergestad EM, Mathiesen G, Nes IF, Holo H. 2011. Transcriptome, proteome, and metabolite analyses of a lactate dehydrogenase-negative mutant of *Enterococcus faecalis* V583. *Appl Environ Microbiol* **77**: 2406–2413.
- Mendoza-Vargas A, Olvera L, Olvera M, Grande R, Vega-Alvarado L, Taboada B, Jimenez-Jacinto V, Salgado H, Juárez K, Contreras-Moreira B, et al. 2009. Genome-wide identification of transcription start sites, promoters and transcription factor binding sites in *E. coli*. *PLoS One* **4**: e7526.
- Mitschke J, Vioque A, Haas F, Hess WR, Muro-Pastor AM. 2011. Dynamics of transcriptional start site selection during nitrogen stress-induced cell differentiation in *Anabaena* sp. PCC7120. *Proc Natl Acad Sci* **108**: 20130–20135.
- Mohanty BK, Kushner SR. 2006. The majority of *Escherichia coli* mRNAs undergo post-transcriptional modification in exponentially growing cells. *Nucleic Acids Res* **34**: 5695–5704.
- Morton T, Petricka J, Corcoran DL, Li S, Winter CM, Carda A, Benfey PN, Ohler U, Megraw M. 2014. Paired-end analysis of transcription start sites in *Arabidopsis* reveals plant-specific promoter signatures. *Plant Cell* **26**: 2746–2760.
- Nakayama J, Chen S, Oyama N, Nishiguchi K, Azab EA, Tanaka E, Kariyama R, Sonomoto K. 2006. Revised model for *Enterococcus faecalis* fsr quorum-sensing system: The small open reading frame fsrD encodes the gelatinase biosynthesis-activating pheromone propeptide corresponding to staphylococcal AgrD. *J Bacteriol* **188**: 8321–8326.
- Nicolas P, Mäder U, Dervyn E, Rochat T, Leduc A, Pigeonneau N, Bidnenko E, Marchadier E, Hoebeke M, Aymerich S, et al. 2012. Condition-dependent transcriptome reveals high-level regulatory architecture in *Bacillus subtilis*. *Science* **335**: 1103–1106.
- Opsata M, Nes I, Holo H. 2011. Class Iia bacteriocin resistance in *Enterococcus faecalis* V583: The mannose PTS operon mediates global transcriptional responses. *BMC Microbiol* **10**: 224.
- Paulsen IT, Banerjee L, Myers GS, Nelson KE, Seshadri R, Read TD, Fouts DE, Eisen JA, Gill SR, Heidelberg JF, et al. 2003. Role of mobile DNA in the evolution of vancomycin-resistant *Enterococcus faecalis*. *Science* **299**: 2071–2074.
- Pedersen MB, Garrigues C, Tuphile K, Brun C, Vido K, Bennedsen M, Møllgaard H, Gaudu P, Gruss A. 2008. Impact of aeration and heme-activated respiration on *Lactococcus lactis* gene expression: identification of a heme-responsive operon. *J Bacteriol* **190**: 4903–4911.
- Pfeiffer T, Schuster S, Bonhoeffer S. 2001. Cooperation and competition in the evolution of ATP-producing pathways. *Science* **292**: 504–507.
- Qin X, Singh KV, Weinstock GM, Murray BE. 2000. Effects of *enterococcus faecalis* fsr genes on production of gelatinase and a serine protease and virulence. *Infect Immun* **68**: 2579–2586.
- Qin X, Singh KV, Weinstock GM, Murray BE. 2001. Characterization of fsr, a regulator controlling expression of gelatinase and serine protease in *Enterococcus faecalis* OG1RF. *J Bacteriol* **183**: 3372–3382.
- Qin J, Li R, Raes J, Arumugam M, Burgdorf KS, Manichanh C, Nielsen T, Pons N, Levenez F, Yamada T, et al. 2010. A human gut microbial gene catalogue established by metagenomic sequencing. *Nature* **464**: 59–65.
- Raabe CA, Tang TH, Brosius J, Rozhddestvensky TS. 2014. Biases in small RNA deep sequencing data. *Nucleic Acids Res* **42**: 1414–1426.
- Rasmussen S, Nielsen HB, Jarmer H. 2009. The transcriptionally active regions in the genome of *Bacillus subtilis*. *Mol Microbiol* **73**: 1043–1057.
- Redon E, Loubière P, Coccain-Bousquet M. 2005. Role of mRNA stability during genome-wide adaptation of *Lactococcus lactis* to carbon starvation. *J Biol Chem* **280**: 36380–36385.
- Repoila F, Darfeuille F. 2009. Small regulatory non-coding RNAs in bacteria: physiology and mechanistic aspects. *Biol Cell* **101**: 117–131.
- Roberts A, Trapnell C, Donaghey J, Rinn JL, Pachter L. 2011. Improving RNA-Seq expression estimates by correcting for fragment bias. *Genome Biol* **12**: R22.
- Robinson MD, Oshlack A. 2010. A scaling normalization method for differential expression analysis of RNA-seq data. *Genome Biol* **11**: R25.
- Rochat T, Bouloc P, Repoila F. 2013. Gene expression control by selective RNA processing and stabilization in bacteria. *FEMS Microbiol Lett* **344**: 104–113.
- Rustad TR, Minch KJ, Brabant W, Winkler JK, Reiss DJ, Baliga NS, Sherman DR. 2013. Global analysis of mRNA stability in *Mycobacterium tuberculosis*. *Nucleic Acids Res* **41**: 509–517.
- Sahm DF, Kissinger J, Gilmore MS, Murray PR, Mulder R, Solliday J, Clarke B. 1989. In vitro susceptibility studies of vancomycin-resistant *Enterococcus faecalis*. *Antimicrob Agents Chemother* **33**: 1588–1591.
- Sayed N, Jousselin A, Felden B. 2012. A cis-antisense RNA acts in trans in *Staphylococcus aureus* to control translation of a human cytolysin peptide. *Nat Struct Mol Biol* **19**: 105–112.
- Schlüter JP, Reinkensmeier J, Daschkey S, Evgueniev-Hackenberg E, Jansen S, Jänicke S, Becker JD, Giegerich R, Becker A. 2010. A genome-wide survey of sRNAs in the symbiotic nitrogen-fixing alpha-proteobacterium *Sinorhizobium meliloti*. *BMC Genomics* **11**: 245.
- Selinger DW, Saxena RM, Cheung KJ, Church GM, Rosenow C. 2003. Global RNA half-life analysis in *Escherichia coli* reveals positional patterns of transcript degradation. *Genome Res* **13**: 216–223.
- Sesto N, Wurtzel O, Archambaud C, Sorek R, Cossart P. 2013. The excludon: a new concept in bacterial antisense RNA-mediated gene regulation. *Nat Rev Microbiol* **11**: 75–82.
- Sharma CM, Hoffmann S, Darfeuille F, Reignier J, Findeiss S, Sittka A, Chabas S, Reiche K, Hackermüller J, Reinhardt R, et al. 2010. The primary transcriptome of the major human pathogen *Helicobacter pylori*. *Nature* **464**: 250–255.

- Shioya K, Michaux C, Kuenne C, Hain T, Verneuil N, Budin-Verneuil A, Hartsch T, Hartke A, Giard JC. 2011. Genome-wide identification of small RNAs in the opportunistic pathogen *Enterococcus faecalis* V583. *PLoS One* **6**: e23948.
- Sittka A, Lucchini S, Papenfort K, Sharma CM, Rolle K, Binnewies TT, Hinton JC, Vogel J. 2008. Deep sequencing analysis of small noncoding RNA and mRNA targets of the global post-transcriptional regulator, Hfq. *PLoS Genet* **4**: e1000163.
- Solheim M, Aakra A, Vebo H, Snipen L, Nes IF. 2007. Transcriptional responses of *Enterococcus faecalis* V583 to bovine bile and sodium dodecyl sulfate. *Appl Environ Microbiol* **73**: 5767–5774.
- Steglich C, Lindell D, Futschik M, Rector T, Steen R, Chisholm SW. 2010. Short RNA half-lives in the slow-growing marine cyanobacterium *Prochlorococcus*. *Genome Biol* **11**: R54.
- Stein LD, Mungall C, Shu S, Caudy M, Mangone M, Day A, Nickerson E, Stajich JE, Harris TW, Arva A, Lewis S. 2002. The generic genome browser: a building block for a model organism system database. *Genome Res* **12**: 1599–1610.
- Thomason MK, Bischler T, Eisenbart SK, Förstner KU, Zhang A, Herbig A, Nieselt K, Sharma CM, Storz G. 2015. Global transcriptional start site mapping using differential RNA sequencing reveals novel antisense RNAs in *Escherichia coli*. *J Bacteriol* **197**: 18–28.
- Toledo-Arana A, Solano C. 2010. Deciphering the physiological blueprint of a bacterial cell: revelations of unanticipated complexity in transcriptome and proteome. *Bioessays* **32**: 461–467.
- Toledo-Arana A, Dussurget O, Nikitas G, Sesto N, Guet-Revillet H, Balestrino D, Loh E, Gripenland J, Tiensuu T, Vaitkevicius K, et al. 2009. The *Listeria* transcriptional landscape from saprophytism to virulence. *Nature* **459**: 950–956.
- Trapnell C, Williams BA, Pertea G, Mortazavi A, Kwan G, van Baren MJ, Salzberg SL, Wold BJ, Pachter L. 2010. Transcript assembly and quantification by RNA-Seq reveals unannotated transcripts and isoform switching during cell differentiation. *Nat Biotechnol* **28**: 511–515.
- Vebo HC, Snipen L, Nes IF, Brede DA. 2009. The transcriptome of the nosocomial pathogen *Enterococcus faecalis* V583 reveals adaptive responses to growth in blood. *PLoS One* **4**: e7660.
- Vebo HC, Solheim M, Snipen L, Nes IF, Brede DA. 2010. Comparative genomic analysis of pathogenic and probiotic *Enterococcus faecalis* isolates, and their transcriptional responses to growth in human urine. *PLoS One* **5**: e12489.
- Verneuil N, Mazé A, Sanguinetti M, Laplace JM, Benachour A, Auffray Y, Giard JC, Hartke A. 2006. Implication of (Mn)superoxide dismutase of *Enterococcus faecalis* in oxidative stress responses and survival inside macrophages. *Microbiology* **152**: 2579–2589.
- Vesić D, Kristich CJ. 2013. A Rex family transcriptional repressor influences H₂O₂ accumulation by *Enterococcus faecalis*. *J Bacteriol* **195**: 1815–1824.
- Wadler CS, Vanderpool CK. 2007. A dual function for a bacterial small RNA: SgrS performs base pairing-dependent regulation and encodes a functional polypeptide. *Proc Natl Acad Sci* **104**: 20454–20459.
- Ward DE, van Der Weijden CC, van Der Merwe MJ, Westerhoff HV, Claiborne A, Snoep JL. 2000. Branched-chain α -keto acid catabolism via the gene products of the *bkd* operon in *Enterococcus faecalis*: a new, secreted metabolite serving as a temporary redox sink. *J Bacteriol* **182**: 3239–3246.
- Waters LS, Storz G. 2009. Regulatory RNAs in bacteria. *Cell* **136**: 615–628.
- Winstedt L, Frankenberg L, Hederstedt L, von Wachenfeldt C. 2000. *Enterococcus faecalis* V583 contains a cytochrome bd-type respiratory oxidase. *J Bacteriol* **182**: 3863–3866.
- Wurtzel O, Sesto N, Mellin JR, Karunker I, Edelheit S, Bécavin C, Archambaud C, Cossart P, Sorek R. 2012. Comparative transcriptomics of pathogenic and non-pathogenic *Listeria* species. *Mol Syst Biol* **8**: 583.
- Yamamoto Y, Pargade V, Lamberet G, Gaudu P, Thomas F, Texereau J, Gruss A, Trieu-Cuot P, Poyart C. 2006. Roles of environmental heme, and menaquinone, in *Streptococcus agalactiae*. *Mol Microbiol* **62**: 772–785.
- Zhuang F, Fuchs RT, Sun Z, Zheng Y, Robb GB. 2012. Structural bias in T4 RNA ligase-mediated 3'-adapter ligation. *Nucleic Acids Res* **40**: e54.



RNA

A PUBLICATION OF THE RNA SOCIETY

Whole-genome mapping of 5' RNA ends in bacteria by tagged sequencing: a comprehensive view in *Enterococcus faecalis*

Nicolas Innocenti, Monica Golumbeanu, Aymeric Fouquier d'Hérouël, et al.

RNA 2015 21: 1018-1030 originally published online March 3, 2015
Access the most recent version at doi:[10.1261/rna.048470.114](https://doi.org/10.1261/rna.048470.114)

Supplemental Material

<http://rnajournal.cshlp.org/content/suppl/2015/02/03/rna.048470.114.DC1>

References

This article cites 90 articles, 30 of which can be accessed free at:
<http://rnajournal.cshlp.org/content/21/5/1018.full.html#ref-list-1>

Creative Commons License

This article is distributed exclusively by the RNA Society for the first 12 months after the full-issue publication date (see <http://rnajournal.cshlp.org/site/misc/terms.xhtml>). After 12 months, it is available under a Creative Commons License (Attribution-NonCommercial 4.0 International), as described at <http://creativecommons.org/licenses/by-nc/4.0/>.

Email Alerting Service

Receive free email alerts when new articles cite this article - sign up in the box at the top right corner of the article or [click here](#).

To subscribe to *RNA* go to:
<http://rnajournal.cshlp.org/subscriptions>
